Materials Advances

ROYAL SOCIETY OF CHEMISTRY

COMMUNICATION

View Article Online
View Journal | View Issue

Check for updates

Cite this: *Mater. Adv.*, 2021, 2, 7842

Received 31st August 2021,
Accepted 4th November 2021

DOI: 10.1039/d1ma00784j

rsc.li/materials-advances

Single-step ball milling synthesis of highly Li^+ conductive $Li_{5.3}PS_{4.3}ClBr_{0.7}$ glass ceramic electrolyte enables low-impedance all-solid-state batteries†

Marvin Cronau, Marvin Szabo and Bernhard Roling *

A single-step high-energy ball milling process was used for the synthesis of a $Li_{5.3}PS_{4.3}ClBr_{0.7}$ glass ceramic. This material exhibits a Li^+ conductivity of 5.2 mS cm^{-1}, the highest value reported so far at room temperature for a Li^+ solid electrolyte pellet prepared without any annealing step. We demonstrate the utilization of this electrolyte in an all-solid-state battery exhibiting a composite cathode impedance of only 5 Ω cm^2 at room temperature.

All-solid-state batteries (ASSBs) have come into focus in recent years as energy storage devices with energy densities potentially exceeding those of conventional lithium-ion batteries (LIBs). However, in practice, severe problems still have to be solved. In order to reach high energy densities, it is indispensable to use lithium as anode and to build composite cathodes with high active material loading in the range of 85 wt%.[1,2] In order to achieve fast ion transport inside the cathode despite the high active material loading, the solid electrolyte should have a high ionic conductivity and should form a continuous phase with low-tortuosity ion transport pathways.

The currently most promising group of SEs are sulphide-based materials. Recently, Lee *et al.* built an ASSB with a capacity retention of over 80% after 1000 cycles using microcrystalline argyrodite-type Li_6PS_5Cl materials as electrolyte.[2] Most sulphide-based SEs are synthesized *via* a two-step or even three-step synthesis. First the starting materials are mixed and pre-treated in a ball mill. Afterwards, the resulting powder is filled into a quartz ampoule, and the quartz ampoule is heated up to a temperature (powder annealing), at which the material is partially crystallized (glass ceramic) or completely crystallised (microcrystalline material). The powder is then ground and pressed to a pellet (cold-pressed pellet), in some cases followed by pellet annealing. Pellet annealing leads usually to a considerable enhancement of the ionic conductivity due to reduced grain boundary resistances.

Department of Chemistry, Philipps-Universität Marburg, Hans-Meerwein-Strasse 4, 35032, Marburg, Germany. E-mail: roling@staff.uni-marburg.de

† Electronic supplementary information (ESI) available. See DOI: 10.1039/d1ma00784j

Argyrodite-type Li_6PS_5Cl reaches ionic conductivity values up to 6 mS cm^{-1} after pellet annealing.[3–16] Although this value is sufficient for building working ASSBs, some pellet-annealed, fully microcrystalline SEs with a significantly higher conductivity have been discovered. One way to increase the Li^+ conductivity is cation doping of the argyrodites. For instance, $Li_{6.6}P_{0.4}Ge_{0.6}S_5I$ exhibits a Li^+ conductivity of 5.4 mS cm^{-1} after powder annealing and cold pressing in comparison to Li_6PS_5I with only 1.3 μS cm^{-1}. After pellet annealing, the conductivity of $Li_{6.6}P_{0.4}Ge_{0.6}S_5I$ increases to 18.4 mS cm^{-1}.[17] $Li_{6.6}Si_{0.6}Sb_{0.4}S_5I$ outperforms $Li_{6.6}P_{0.4}Ge_{0.6}S_5I$ with 14.8 mS cm^{-1} for the cold-pressed pellet and 24 mS cm^{-1} for the annealed pellet.[18] However, materials containing tetrel atoms are chemically less stable than the parent compound Li_6PS_5Cl.[19–21]

Another promising approach to boost the Li^+ conductivity is the synthesis of halide-rich $Li_{6-x}PS_{5-x}Hal_{1+x}$ (Hal = Cl, Br) solid electrolytes.[22,23] For example, the reported Li^+ conductivities of $Li_{5.5}PS_{4.5}Cl_{1.5}$ and $Li_{5.5}PS_{4.5}Br_{1.5}$ after pellet annealing reach values of about 11 and 12 mS cm^{-1}, respectively, while the conductivity of the recently synthesized mixed-halide microcrystalline argyrodite $Li_{5.3}PS_{4.3}ClBr_{0.7}$ reaches 24 mS cm^{-1}.[24–27]

In general, two-step or three-step syntheses are well suited for lab-scale production, but not for commercial large-scale production.[28] Furthermore, high-temperature annealing (around 500–600 °C) of SE particles inside the composite electrodes of ASSBs is not possible due to the limited thermal stability of active material particles, like NMC.[29] Therefore, the development of highly conductive SE materials, which reach high ionic conductivities without using high-temperature annealing steps during synthesis is of utmost importance.

Herein, we present a single-step ball milling synthesis of a glass ceramic (GC) $Li_{5.3}PS_{4.3}ClBr_{0.7}$ powder. After cold pressing, the resulting pellet reaches the highest Li^+ conductivity reported so far for Li^+ solid electrolytes prepared without any annealing step. The simple synthesis in comparison to the materials mentioned above, see Fig. 1, and the already demonstrated long-term stability of glass ceramic solid electrolytes in ASSBs[30] makes GC $Li_{5.3}PS_{4.3}ClBr_{0.7}$ a viable candidate for the

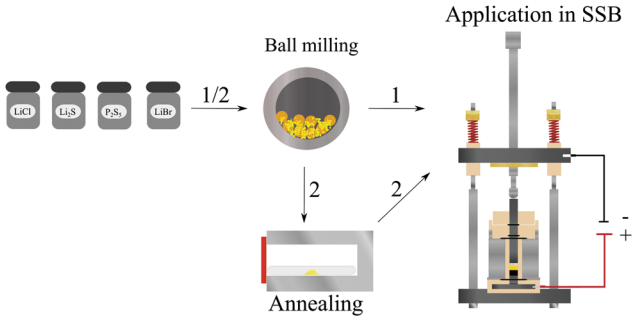

Fig. 1 Illustration of different synthesis routes for solid electrolytes and of a home-made cell setup for the characterisation of all solid-state batteries (ASSBs).

use in ASSBs. We demonstrate that the integration of GC $Li_{5.3}PS_{4.3}ClBr_{0.7}$ into an In/$LiCoO_2$ solid-state battery leads to remarkably low cathode impedance and overall battery impedances.

Stoichiometric amounts of the precursors were filled into a zirconia pot with 10 zirconia balls (10 mm diameter) and ball milled for 8.25 hours (850 rpm). In the case of argyrodites, this synthesis route leads in general to nanocrystallites in an amorphous matrix, with low volume fractions of the amorphous phase in the range of 10–15 vol%.[27,31–33] The resulting powder (Fig. 2) was used as received without any heat treatment (a detailed description of the synthesis can be found in the ESI†). The X-ray powder diffractogram shows the typical nanocrystalline pattern (average particle size about 18 nm) of many argyrodite-type glass ceramic electrolytes.

For the fabrication of pellets for Li^+ conductivity measurements, a fabrication pressure of 490 MPa was used inside a CompreDrive laboratory press (rhd instruments, Darmstadt, Germany). The impedance measurements were carried out by means of an Autolab PGSTAT302N (Metrohm Autolab, Utrecht, Netherlands) under an applied stack pressure of 100 MPa. The impedance spectra were taken in a frequency range from 10^5–10^1 Hz and in a temperature range from 30–85 °C with an applied rms AC voltage of 10 mV. Since reported Li^+ conductivity values depend strongly on the fabrication pressure and stack pressure, we used identical pressure conditions for the fabrication of four solid electrolyte pellets and the subsequent ionic conductivity measurements. These solid electrolytes are: (i) GC Li_6PS_5Cl prepared by a single-step ball milling

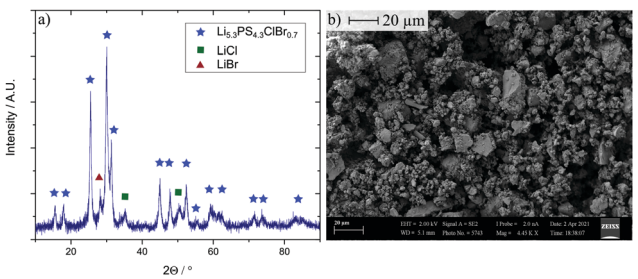

Fig. 2 (a) X-Ray diffraction pattern of the SE. (b) Scanning electron microscopy image (magnification: 5000) of the synthesized powder.

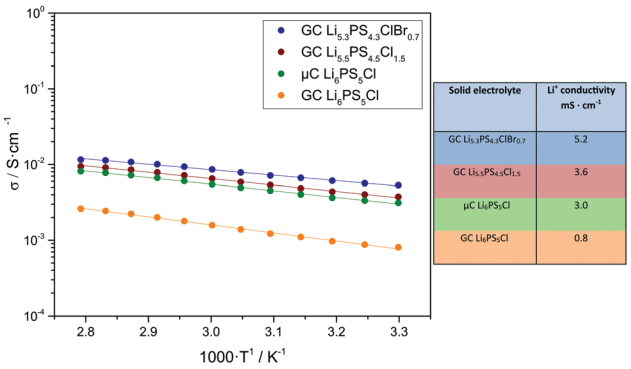

Fig. 3 Arrhenius plots of the Li^+ conductivity σ of different solid electrolytes (left, temperature range 30 to 85 °C) and table with Li^+ ionic conductivity at 30 °C (right).

synthesis; (ii) microcrystalline (µC) Li_6PS_5Cl with applied powder annealing at 550 °C; (iii) GC $Li_{5.5}PS_{4.5}Cl_{1.5}$ prepared by a single-step ball milling synthesis; (iv) GC $Li_{5.3}PS_{4.3}ClBr_{0.7}$ prepared by a single-step ball milling synthesis.

Fig. 3 shows an Arrhenius plot of the Li^+ conductivity of all materials at 30 °C. With 5.2 mS cm^{-1}, the ionic conductivity of $Li_{5.3}PS_{4.3}ClBr_{0.7}$ clearly exceeds those of the other materials, and even that of powder-annealed Li_6PS_5Cl.

To demonstrate the performance of the new glass ceramic $Li_{5.3}PS_{4.3}ClBr_{0.7}$ electrolyte in an ASSB, the electrolyte was used for the preparation of the separator layer as well as for the preparation of composite cathodes with $LiNbO_3$-coated $LiCoO_2$ active material particles and carbon fibers as conductive additive (70 : 30 : 3 wt%). Indium foil was used as anode, which was pressed for one minute with 298 MPa onto the separator layer to form a good anode/separator contact. The lab-scale ASSB was characterized in a home-made cell setup with pressure control, see Fig. 1. For the battery cycling experiments, a pressure of 98 MPa was applied, and the battery was cycled at room temperature with a rate of 0.1 C between the cutoff voltages 2.1 V and 3.7 V. Fig. 4(a) shows the first charge and the first discharge voltage profile of the battery. With a discharge capacity of 147 mA h g^{-1}, the battery exploits the full capacity of $LiCoO_2$. For comparison, an ASSB was built with non-annealed Li_6PS_5Cl in the composite cathode and in the separating SE layer, which reaches only a capacity of 137 mA h g^{-1}.

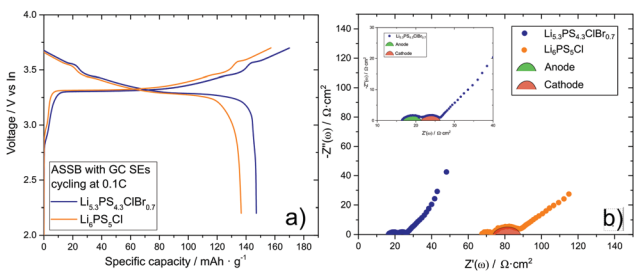

Fig. 4 (a) Voltage profiles of the first charge and the first discharge cycle of an ASSB utilizing the new $Li_{5.3}PS_{4.3}ClBr_{0.7}$ glass ceramic in comparison to a ASSB using less conductive glass ceramic Li_6PS_5Cl. (b) Impedance spectra of both batteries after the first charge cycle.

Impedance spectra of the two ASSBs after the first discharge cycle are shown in Fig. 4(b). The higher ionic conductivity of GC $Li_{5.3}PS_{4.3}ClBr_{0.7}$ as compared to GC Li_6PS_5Cl manifest in a lower high-frequency resistance of the GC $Li_{5.3}PS_{4.3}ClBr_{0.7}$-based battery, which can be identified with the separator resistance, and in a smaller second semicircle, which is usually attributed to the cathode impedance. The cathode impedance is determined by the ion transport resistance of the solid electrolyte within the composite cathode as well as by the charge transfer resistance at the interfaces between the active material particles and the solid electrolyte particles.[34] The fast ion transport in the GC $Li_{5.3}PS_{4.3}ClBr_{0.7}$-based cathode leads to a cathode impedance value of only 5 Ω cm^2, which is one of the lowest values reported so far at room temperature.[35]

In conclusion, we synthesized the glass ceramic $Li_{5.3}PS_{4.3}ClBr_{0.7}$ electrolyte in a single-step synthesis without any annealing step and integrated this electrolyte in a low-impedance ASSB. To our knowledge, cold-pressed GC $Li_{5.3}PS_{4.3}ClBr_{0.7}$ exhibits the highest Li^+ conductivity (5.2 mS cm^{-1}) reported so far for electrolytes prepared without annealing steps and surpasses that of annealed microcrystalline Li_6PS_5Cl (3 mS cm^{-1}). The cathode impedance of our lab-scale ASSB was only 5 Ω cm^2, one of lowest values achieved so far at room temperature. Using a thinner GC $Li_{5.3}PS_{4.3}ClBr_{0.7}$-based separator layer would further lower the total impedance to values of 30–40 Ω cm^2. Building an ASSB with an area of some 1000 cm^2, like in commercial Li^+ ion batteries,[36] would then result in a battery resistance in the range of 10 mΩ, which is similar to that of such commercial Li^+ ion batteries. Together with the already reported favourable pressure-dependent properties,[37] and the high long-term stability of glass ceramic SE in ASSBs,[30] our results give strong indication that GC $Li_{5.3}PS_{4.3}ClBr_{0.7}$ prepared by a simple one-step synthesis is a viable candidate for next-generation batteries. In future work, milling protocols for reducing the energy consumption should be developed, *e.g.* by reducing the rotational speed and by using balls with optimized diameter.

Conflicts of interest

There are no conflicts to declare.

Acknowledgements

We thank Toyota Motor Corporation for providing $LiCoO_2$.

References

1 J. Janek and W. G. Zeier, A solid future for battery development, *Nat. Energy*, 2016, **1**, 16141.
2 Y.-G. Lee, S. Fujiki, C. Jung, N. Suzuki, N. Yashiro, R. Omoda, D.-S. Ko, T. Shiratsuchi, T. Sugimoto, S. Ryu, J. H. Ku, T. Watanabe, Y. Park, Y. Aihara, D. Im and I. T. Han, High-energy long-cycling all-solid-state lithium metal batteries enabled by silver–carbon composite anodes, *Nat. Energy*, 2020, **5**, 299–308.
3 S. Boulineau, M. Courty, J.-M. Tarascon and V. Viallet, Mechanochemical synthesis of Li-argyrodite Li_6PS_5X (X = Cl, Br, I) as sulfur-based solid electrolytes for all solid-state batteries application, *Solid State Ionics*, 2012, **221**, 1–5.
4 S. Choi, J. Ann, J. Do, S. Lim, C. Park and D. Shin, Application of Rod-Like Li_6PS_5Cl Directly Synthesized by a Liquid Phase Process to Sheet-Type Electrodes for All-Solid-State Lithium Batteries, *J. Electrochem. Soc.*, 2019, **166**, A5193–A5200.
5 J.-M. Doux, Y. Yang, D. H. S. Tan, H. Nguyen, E. A. Wu, X. Wang, A. Banerjee and Y. S. Meng, Pressure effects on sulfide electrolytes for all solid-state batteries, *J. Mater. Chem. A*, 2020, **8**, 5049–5055.
6 G. Liu, W. Weng, Z. Zhang, L. Wu, J. Yang and X. Yao, Densified Li_6PS_5Cl Nanorods with High Ionic Conductivity and Improved Critical Current Density for All-Solid-State Lithium Batteries, *Nano Lett.*, 2020, **20**, 6660–6665.
7 P. R. Rayavarapu, N. Sharma, V. K. Peterson and S. Adams, Variation in structure and Li^+-ion migration in argyrodite-type Li_6PS_5X (X = Cl, Br, I) solid electrolytes, *J. Solid State Electrochem.*, 2012, **16**, 1807–1813.
8 N. C. Rosero-Navarro, A. Miura and K. Tadanaga, Preparation of lithium ion conductive Li_6PS_5Cl solid electrolyte from solution for the fabrication of composite cathode of all-solid-state lithium battery, *J. Sol-Gel Sci. Technol.*, 2019, **89**, 303–309.
9 S. Wang, Y. Zhang, X. Zhang, T. Liu, Y.-H. Lin, Y. Shen, L. Li and C.-W. Nan, High-Conductivity Argyrodite Li_6PS_5Cl Solid Electrolytes Prepared *via* Optimized Sintering Processes for All-Solid-State Lithium–Sulfur Batteries, *ACS Appl. Mater. Interfaces*, 2018, **10**, 42279–42285.
10 M. Xuan, W. Xiao, H. Xu, Y. Shen, Z. Li, S. Zhang, Z. Wang and G. Shao, Ultrafast solid-state lithium–ion conductor through alloying induced lattice softening of Li_6PS_5Cl, *J. Mater. Chem. A*, 2018, **6**, 19231–19240.
11 C. Yu, S. Ganapathy, J. Hageman, L. van Eijck, E. R. H. van Eck, L. Zhang, T. Schwietert, S. Basak, E. M. Kelder and M. Wagemaker, Facile Synthesis toward the Optimal Structure-Conductivity Characteristics of the Argyrodite Li_6PS_5Cl Solid-State Electrolyte, *ACS Appl. Mater. Interfaces*, 2018, **10**, 33296–33306.
12 C. Yu, L. van Eijck, S. Ganapathy and M. Wagemaker, Synthesis, structure and electrochemical performance of the argyrodite Li_6PS_5Cl solid electrolyte for Li–ion solid state batteries, *Electrochim. Acta*, 2016, **215**, 93–99.
13 S. Yubuchi, S. Teragawa, K. Aso, K. Tadanaga, A. Hayashi and M. Tatsumisago, Preparation of high lithium-ion conducting Li_6PS_5Cl solid electrolyte from ethanol solution for all-solid-state lithium batteries, *J. Power Sources*, 2015, **293**, 941–945.
14 J. Zhang, H. Zhong, C. Zheng, Y. Xia, C. Liang, H. Huang, Y. Gan, X. Tao and W. Zhang, All-solid-state batteries with slurry coated $LiNi_{0.8}Co_{0.1}Mn_{0.1}O2$ composite cathode and Li_6PS_5Cl electrolyte: Effect of binder content, *J. Power Sources*, 2018, **391**, 73–79.
15 Y. J. Nam, D. Y. Oh, S. H. Jung and Y. S. Jung, Toward practical all-solid-state lithium-ion batteries with high

energy density and safety: Comparative study for electrodes fabricated by dry- and slurry-mixing processes, *J. Power Sources*, 2018, **375**, 93–101.

16 D. H. Kim, D. Y. Oh, K. H. Park, Y. E. Choi, Y. J. Nam, H. A. Lee, S.-M. Lee and Y. S. Jung, Infiltration of Solution-Processable Solid Electrolytes into Conventional Li–Ion-Battery Electrodes for All-Solid-State Li-Ion Batteries, *Nano Lett.*, 2017, **17**, 3013–3020.

17 M. A. Kraft, S. Ohno, T. Zinkevich, R. Koerver, S. P. Culver, T. Fuchs, A. Senyshyn, S. Indris, B. J. Morgan and W. G. Zeier, Inducing High Ionic Conductivity in the Lithium Superionic Argyrodites $Li_{6+x}P_{1-x}Ge_xS_5I$ for All-Solid-State Batteries, *J. Am. Chem. Soc.*, 2018, **140**, 16330–16339.

18 L. Zhou, A. Assoud, Q. Zhang, X. Wu and L. F. Nazar, New Family of Argyrodite Thioantimonate Lithium Superionic Conductors, *J. Am. Chem. Soc.*, 2019, **141**, 19002–19013.

19 S. Wenzel, S. Randau, T. Leichtweiß, D. A. Weber, J. Sann, W. G. Zeier and J. Janek, Direct Observation of the Interfacial Instability of the Fast Ionic Conductor $Li_{10}GeP_2S_{12}$ at the Lithium Metal Anode, *Chem. Mater.*, 2016, **28**, 2400–2407.

20 Y. Kato, S. Hori, T. Saito, K. Suzuki, M. Hirayama, A. Mitsui, M. Yonemura, H. Iba and R. Kanno, High-power all-solid-state batteries using sulfide superionic conductors, *Nat. Energy*, 2016, **1**, 16030.

21 P. Bron, B. Roling and S. Dehnen, Impedance characterization reveals mixed conducting interphases between sulfidic superionic conductors and lithium metal electrodes, *J. Power Sources*, 2017, **352**, 127–134.

22 P. Adeli, J. D. Bazak, K. H. Park, I. Kochetkov, A. Huq, G. R. Goward and L. F. Nazar, Boosting Solid-State Diffusivity and Conductivity in Lithium Superionic Argyrodites by Halide Substitution, *Angew. Chem., Int. Ed.*, 2019, **58**, 8681–8686.

23 Z. Zhang, L. Wu, D. Zhou, W. Weng and X. Yao, Flexible Sulfide Electrolyte Thin Membrane with Ultrahigh Ionic Conductivity for All-Solid-State Lithium Batteries, *Nano Lett.*, 2021, **21**, 5233–5239.

24 P. Wang, H. Liu, S. Patel, X. Feng, P.-H. Chien, Y. Wang and Y.-Y. Hu, Fast Ion Conduction and Its Origin in $Li_{6-x}PS_{5-x}Br_{1+x}$, *Chem. Mater.*, 2020, **32**, 3833–3840.

25 X. Feng, P.-H. Chien, Y. Wang, S. Patel, P. Wang, H. Liu, M. Immediato-Scuotto and Y.-Y. Hu, Enhanced ion conduction by enforcing structural disorder in Li-deficient argyrodites $Li_{6-x}PS_{5-x}Cl_{1+x}$, *Energy Storage Mater.*, 2020, **30**, 67–73.

26 S. V. Patel, S. Banerjee, H. Liu, P. Wang, P.-H. Chien, X. Feng, J. Liu, S. P. Ong and Y.-Y. Hu, Tunable Lithium-Ion Transport in Mixed-Halide Argyrodites $Li_{6-x}PS_{5-x}ClBr_x$: An Unusual Compositional Space, *Chem. Mater.*, 2021, **33**, 1435–1443.

27 W. D. Jung, J.-S. Kim, S. Choi, S. Kim, M. Jeon, H.-G. Jung, K. Y. Chung, J.-H. Lee, B.-K. Kim, J.-H. Lee and H. Kim, Superionic Halogen-Rich Li-Argyrodites Using *In Situ* Nanocrystal Nucleation and Rapid Crystal Growth, *Nano Lett.*, 2020, **20**, 2303–2309.

28 J. Wu, S. Liu, F. Han, X. Yao and C. Wang, Lithium/Sulfide All-Solid-State Batteries using Sulfide Electrolytes, *Adv. Mater.*, 2021, **33**, 2000751.

29 H. Konishi, T. Yuasa and M. Yoshikawa, Thermal stability of $Li_{1-y}Ni_xMn_{(1-x)/2}Co_{(1-x)/2}O_2$ layer-structured cathode materials used in Li–Ion batteries, *J. Power Sources*, 2011, **196**, 6884–6888.

30 S. Wang, W. Zhang, X. Chen, D. Das, R. Ruess, A. Gautam, F. Walther, S. Ohno, R. Koerver, Q. Zhang, W. G. Zeier, F. H. Richter, C.-W. Nan and J. Janek, Influence of Crystallinity of Lithium Thiophosphate Solid Electrolytes on the Performance of Solid-State Batteries, *Adv. Energy Mater.*, 2021, 2100654.

31 P. Heitjans, M. Masoud, A. Feldhoff and M. Wilkening, NMR and impedance studies of nanocrystalline and amorphous ion conductors: lithium niobate as a model system, *Faraday Discuss.*, 2007, **134**, 67–82.

32 D. Prutsch, S. Breuer, M. Uitz, P. Bottke, J. Langer, S. Lunghammer, M. Philipp, P. Posch, V. Pregartner, B. Stanje, A. Dunst, D. Wohlmuth, H. Brandstätter, W. Schmidt, V. Epp, A. Chadwick, I. Hanzu and M. Wilkening, Nanostructured Ceramics: Ionic Transport and Electrochemical Activity, *Z. Phys. Chem.*, 2017, **231**(7-8), 1361–1405.

33 M. Wilkening, V. Epp, A. Feldhoff and P. Heitjans, Tuning the Li Diffusivity of Poor Ionic Conductors by Mechanical Treatment: High Li Conductivity of Strongly Defective $LiTaO_3$ Nanoparticles, *J. Phys. Chem. C*, 2008, **112**, 9291–9300.

34 M. Kroll, M. Duchardt, S. L. Karstens, S. Schlabach, F. Lange, J. Hochstrasser, B. Roling and U. Tallarek, Sheet-type all-solid-state batteries with sulfidic electrolytes: Analysis of kinetic limitations based on a cathode morphology study, *J. Power Sources*, 2021, **505**, 230064.

35 Y. Han, S. H. Jung, H. Kwak, S. Jun, H. H. Kwak, J. H. Lee, S.-T. Hong and Y. S. Jung, Single- or Poly-Crystalline Ni-Rich Layered Cathode, Sulfide or Halide Solid Electrolyte: Which Will be the Winners for All-Solid-State Batteries?, *Adv. Energy Mater.*, 2021, **11**, 2100126.

36 F. Sälzer, L. Pateras Pescara, F. Franke, C. Müller, J. Winkler, M. Schwalm and B. Roling, Assessing the Ion Transport Properties of Highly Concentrated Non-Flammable Electrolytes in a Commercial Li–Ion Battery Cell, *Batteries Supercaps*, 2020, **3**, 117–125.

37 M. Cronau, M. Szabo, C. König, T. B. Wassermann and B. Roling, How to Measure a Reliable Ionic Conductivity? The Stack Pressure Dilemma of Microcrystalline Sulfide-Based Solid Electrolytes, *ACS Energy Lett.*, 2021, **6**, 3072–3077.